Supplementary Information (SI) for Chemical Science.

Dopant-Free Stabilization of Ruthenium Oxide via Metallic Ru-Induced d-Orbital Modulation for Acidic Water Electrolysis

Lei Tan,[a] Meharban Faiza,[a] Jin Tian,[a] Lingzhi Zhu,[a] Tiantian Su,[a] Xiaotong Wu,[a] Yujie Song,[a] Qiuju Zhang,[b] Jingsan Xu,[c] Chao Lin,[a] Xiaopeng Li,*[a] Wei Luo[a]*

[a] State Key Laboratory of Advanced Fibers Materials, College of Materials Science and Engineering, Donghua University, Shanghai 201620, P. R. China

[b] Key Laboratory of Advanced Fuel Cells and Electrolyzers Technology, Ningbo Institute of Material Technology and Engineering, Chinese Academy of Sciences, Ningbo, Zhejiang, 315201, China

[c] School of Chemistry and Physics & Centre for Materials Science, Queensland University of Technology, Brisbane, QLD 4001, Australia

E-mail: linc@dhu.edu.cn; xiaopeng.li@dhu.edu.cn

Experimental section

***Chemicals and materials**:* Sulfuric acid (H_2SO_4, 95-98%), and Sodium Hydroxide (NaOH, ≥96%) were bought from Sinopharm Chemical Reagent Co., Ltd. Sodium Tetrahydroborate ($NaBH_4$. 98%), and Ruthenium (III) Chloride ($RuCl_3$, 99.5%) were supplied by Shanghai Titan Scientific Co., Ltd. Water-^{18}O ($H_2{}^{18}O$, RG, 98 atom % ^{18}O) was purchased from Adamas. Nafion perfluorinated resin solution (5 wt%) and commercial ruthenium oxide (Com-RuO_2) were purchased from Sigma-Aldrich. Both the Hyproof HPM-2080X perfluorosulfonic acid membrane (thickness 80 ± 2.5 μm; proton conductivity: 81 mS cm^{-1}; reinforcement material: expanded polytetrafluoroethylene, ePTFE) and the perfluorosulfonic acid-type ionomer (HCD-1810WB; solid content: 10.08%; density: 883 g mol^{-1}; viscosity: 10.73 mPa·s^{-1}) were purchased from Hancheng Technology Development Co., Ltd. The commercial 60 wt% Pt/C catalyst was sourced from Hydrogen Electric Zhongke New Energy Equipment Co., Ltd. Carbon paper (CP, TGP-H-060, 30% hydrophobic) was sourced from Suzhou Sinero Technology Co. Ltd. Milli-Q water (resistivity: 18.2 ΩM cm^{-1}) was used throughout the experiments. All reagents were of analytical grade and used without further purification.

Synthesis of Ru/RuO$_2$: Ru/RuO_2 was synthesized by dissolving 0.5 mmol $NaBH_4$ in a 0.125 M NaOH aqueous solution, which was then added to a 10 mL 5 mg mL^{-1} $RuCl_3$ solution. The mixture was allowed to react at room temperature for 3 minutes. The resulting black precipitates were separated by centrifugation, washed with water to bring it to neutral pH, and subsequently frozen using liquid nitrogen. The frozen sample was transferred to a freeze dryer and dried for a minimum of 24 hours. Finally, Ru/RuO_2 was obtained by annealing the dried sample at 300 °C for 1 hour in air.

Synthesis of RuO_2: The synthesis of RuO_2 follows a similar procedure to that of Ru/RuO_2, with the primary distinction being the use of a higher annealing temperature of 600 °C.

Chemical and structural characterization: Transmission electron microscopy (TEM) and high-angle annular dark field scanning transmission electron microscopy (HAADF-STEM) were performed using a Talos F200S instrument, with energy-dispersive spectroscopy (EDS) conducted on the same instruement. Powder X-ray diffraction (XRD) was acquired using a Rigaku Miniflex diffractometer equipped with Cu-Kα radiation ($\lambda = 0.154$ nm) at a scan rate of 8º min^{-1}. Nitrogen adsorption isotherms were measured on a Quantachrome Autosorb-iQ at 77 K following degassing at 180 °C for 8 hours. X-ray absorption fine structure (XAFS) spectra of the Ru K-edge were recorded at BL 20U of the Shanghai Synchrotron Radiation Facility (SSRF), with data analysis performed using ATHENA software.[1] X-ray absorption spectra (XAS) of the Ru M-edge and O K-edge were collected at BL02B of the SSRF. X-ray photoelectron spectroscopy (XPS) was conducted using an Escalab 250Xi system, referencing binding energies to C 1s at 284.8 eV.

Electrochemical measurements: Electrochemical measurements were conducted using a CHI 760E electrochemical workstation at room temperature with a 0.5 M H_2SO_4

electrolyte. A $Hg/HgSO_4$ electrode was used as the reference, and a platinum sheet served as the counter electrode. For ink preparation, 2.0 mg Ru/RuO_2 was dispersed in 200 μL mixed solvent (deionized water: ethanol = 1:3.5, v/v) containing 20 μL 5 wt% Nafion as binder, then sonicated for at least 60 min to form a homogeneous ink. Next, 20 μL ink was evenly dropped onto each side of a pre-cleaned 1×1 cm^2 CP allowed to dry completely at room temperature. The mass loadings of the electrocatalysts were optimized approximately 0.4 mg cm^{-2} on CP, which acted as the working electrode for activity and stability tests. Linear sweep voltammetry (LSV) was performed at a scan rate of 5 mV s^{-1}. All potentials were referenced to the Reversible Hydrogen Electrode (RHE), with manual iR correction applied using the formula ($E_{RHE} = E_{Hg/HgSO4} + 0.652$ V + 0.059pH – iR), where i is the current, and R is the uncompensated resistance, determined via electrochemical impedance spectroscopy (EIS). EIS measurements were taken over a frequency range of 100 kHz to 0.1 Hz with an amplitude of 5 mV at 1.5 V vs. RHE. Tafel plots were derived by fitting the polarization curves between the overpotential (η) and log current density (log j) using the equation: $\eta = b\log(j) + a$, where b is the Tafel slope. Double-layer capacitance (C_{dl}) was calculated from cyclic voltammetry (CV) curves in the no-Faradaic region (1.052 to 1.152 V vs. RHE) at varying scan rates. The electrochemically active surface area (ECSA) was determined by ECSA = C_{dl}/C_s, with C_s set to 35 μF cm^{-2}. Long-term durability was evaluated by chronopotentiometry at 10 mA cm^{-2}.

The membrane electrode assembly (MEA) for proton exchange membrane water electrolysis (PEMWE) was engineered using a catalyst-coated membrane (CCM) architecture. Anode catalysts comprising Ru/RuO_2 were deposited on a Hyproof HPM-2080X perfluorosulfonic acid membrane (80 μm thickness, 2*2 cm^2 active area) via spray coating, while for cathode a commercial Pt/C catalyst (60 wt% Pt) was used. The ink recipe and fabrication protocol for MEA are completely different from those for CP-based deposition: we dispersed 10 mg catalyst in a mixed solvent consisting of 0.53 g isopropanol and 0.53 g deionized water, then added 0.06 g of a 10 wt% binder solution (with the same composition as the PEM used in the electrolyzer) before sonicating the mixture for at least 2 hours to form a uniformly dispersed catalyst ink. Afterward, we loaded the entire volume of the prepared catalyst ink into an airbrush and uniformly sprayed it onto both sides of a dry proton exchange membrane. Specifically, the mass loadings of both the anode and cathode catalysts in the PEMWE device are ~2 $mg \cdot cm^{-2}$. The ionomer content in the slurry was approximately 37.5 wt%. The CCM was assembled through hot-pressing (1.0 ton, 140 °C, 3 minutes) to optimize catalyst-membrane interfacial contact. The MEA was assembled using titanium porous transport layers (PTLs) with 350 μm PTFE gaskets ensuring hermetic sealing. Electrochemical testing was conducted in a zero-gap configuration with deionized water anode feed (50 mL min^{-1}, 70 °C), utilizing a recirculating thermal bath to maintain isothermal conditions. LSV curves were recorded at a scan rate of 10 mV s^{-1}, and system durability was assessed at a current density of 1.0 A cm^{-2}.

Operando DEMS measurement: The operando DEMS measurement involves two key stages. In the DEMS setup, a three-electrode configuration was employed where Ru/RuO_2 was drop-casted onto a gold film, which was then deposited on a porous polytetrafluoroethylene substrate as the working electrode. A platinum wire and an Ag/AgCl electrode functioned as the counter and the reference electrodes, respectively. Initially, LSV was performed using a 0.5 M H_2SO_4 electrolyte prepared with $H_2{}^{18}O$ to label the electrocatalyst surface with isotopic water. During this phase, a mass spectrometer was used to detect the gas products, specifically $^{32}O_2$, $^{34}O_2$, and $^{36}O_2$. Subsequently, the ^{18}O-labeled catalyst was tested in 0.5 M H_2SO_4 electrolyte prepared with $H_2{}^{16}O$, while the mass spectrometer continued to monitor the same gas products.

***Theoretical calculations**:* The computational simulations were performed using density functional theory (DFT) within the Vienna ab-initio Simulation Package (VASP). The projector-augmented wave (PAW) method was applied to model the ionic cores, with the Perdew-Burke-Ernzerhof (PBE) functional under the generalized gradient approximation (GGA) for electronic exchange-correlation. A plane wave energy cutoff of 450 eV was employed, and the Brillouin zone was sampled using a 2×2×1 k-point grid centered at the Gamma point. To minimize layer interactions, a 15 Å vacuum was introduced in the vertical direction. Convergence criteria for force and energy were set to 0.05 eV/Å and 10^{-4} eV, respectively. The Ru/RuO_2 model comprises a two-layer rutile RuO_2 structure with a metallic Ru particle, with all layers fully relaxed. Van der Waals interactions were modeled using Grimme's DFT-D3 correction, with dipole corrections applied along the surface normal.[2] Magnetic moment relaxations were permitted (ISPIN=2) during the DFT calculations to accommodate electronic structure changes during optimization. The VASP implicit solvent model was used to simulate water effects. The Gibbs free energy change (ΔG) for the electrochemical oxygen evolution reaction (OER) was computed using the Nørskov et al. approach:[3]

$$\Delta G = \Delta E_{abs} + \Delta E_{ZPE} - T\Delta S + \Delta G_U + \Delta G_{pH}$$

Here, ΔE_{abs} represents the reaction energy from DFT calculations, accounting for the enthalpic change due to adsorption. ΔE_{ZPE} and ΔS are the differences in zero-point energy and entropy between the adsorbed state and the gas phase at 298.15 K. ΔG_U incorporates the contribution of the applied electrode potential (U), set to 1.23 V, while ΔG_{pH} accounts for the free energy correction due to pH variations.

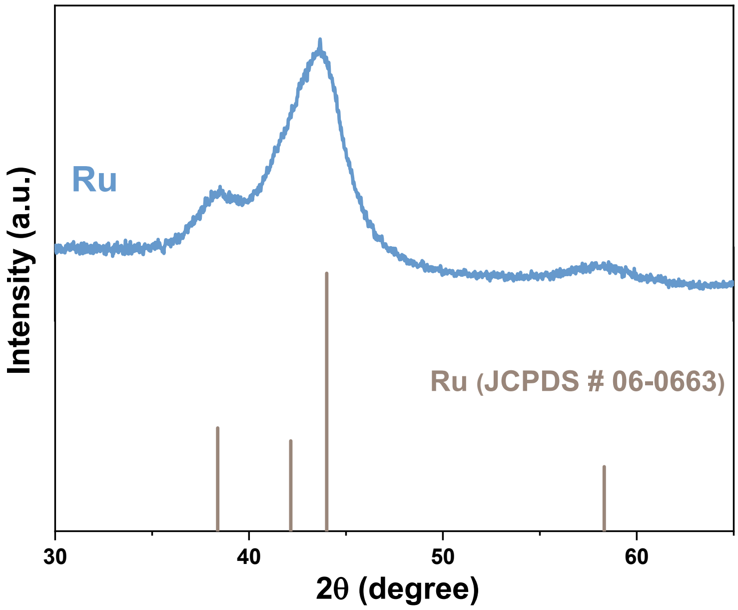

Figure S1. XRD pattern of Ru precursor.

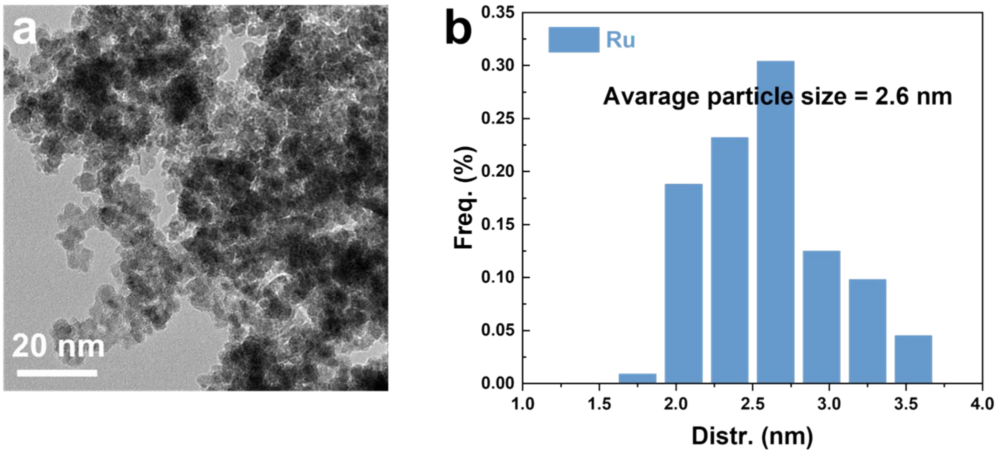

Figure S2. (a) The TEM image and (b) particle size distribution of Ru precursor.

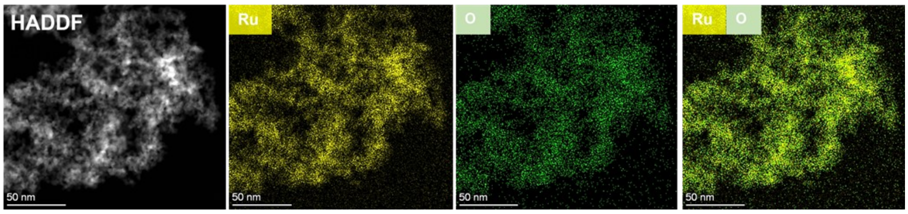

Figure S3. STEM and EDS mapping images of Ru precursor.

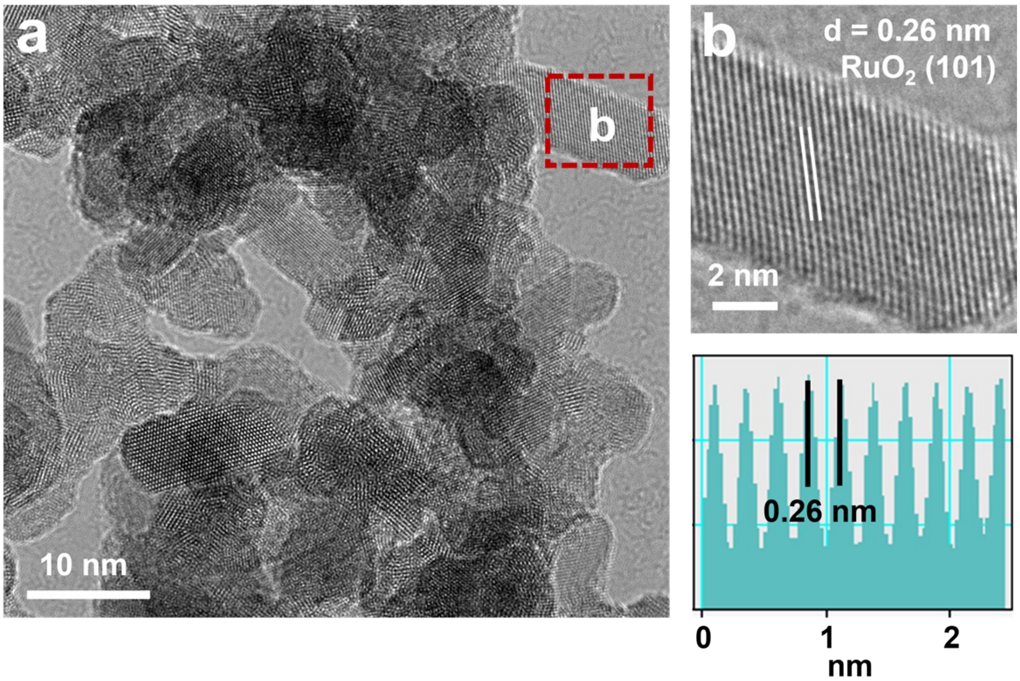

Figure S4. The HR-TEM images of Ru/RuO_2.

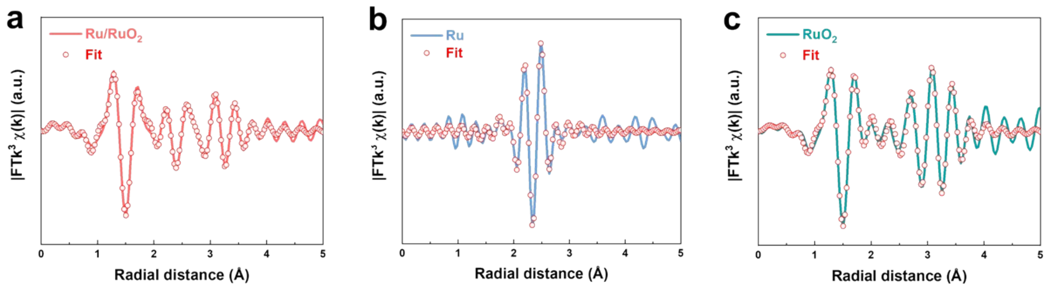

Figure S5. Ru K-edge EXAFS fitting analyses for Ru/RuO_2, Ru foil, and RuO_2.

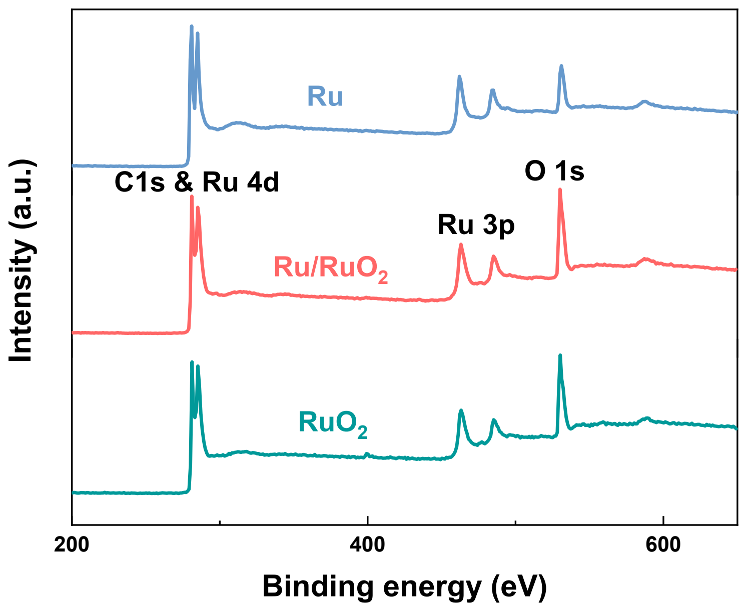

Figure S6. XPS survey spectra of metallic Ru, Ru/RuO_2 and RuO_2.

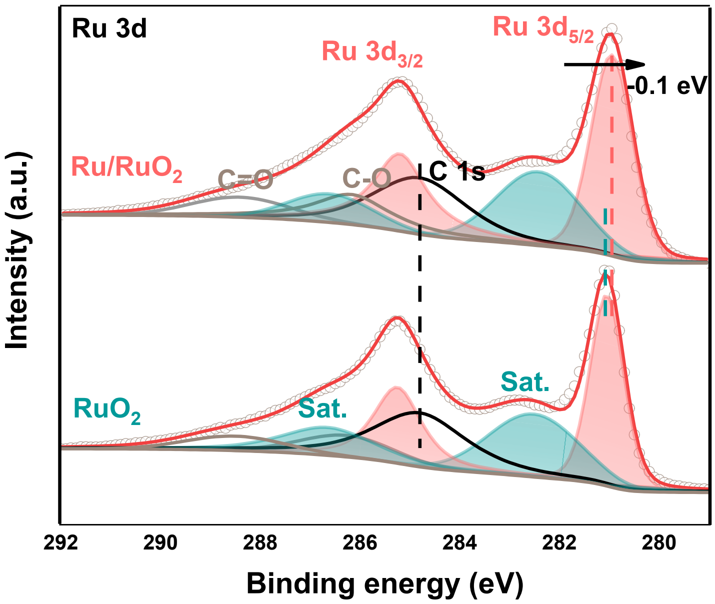

Figure S7. High-resolution XPS spectra of Ru 3d of metallic Ru, Ru/RuO_2, and RuO_2.

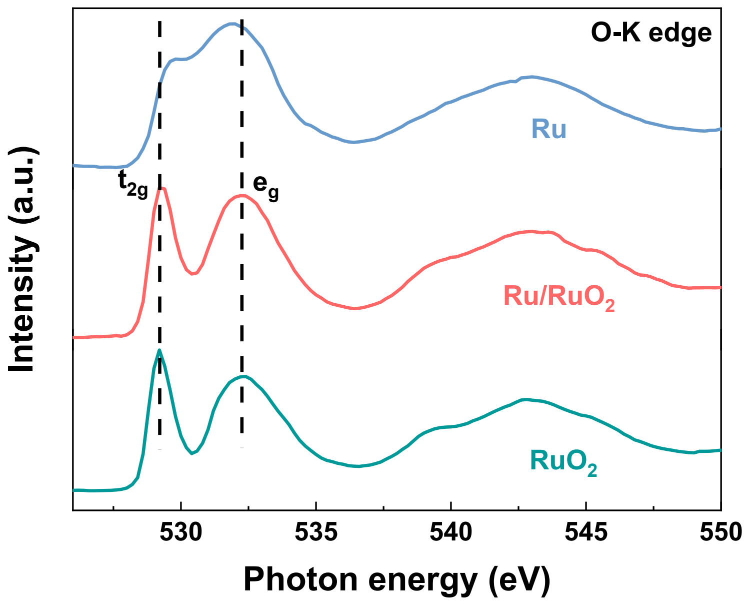

Figure S8. O K-edge spectra of metallic Ru, Ru/RuO_2 and RuO_2.

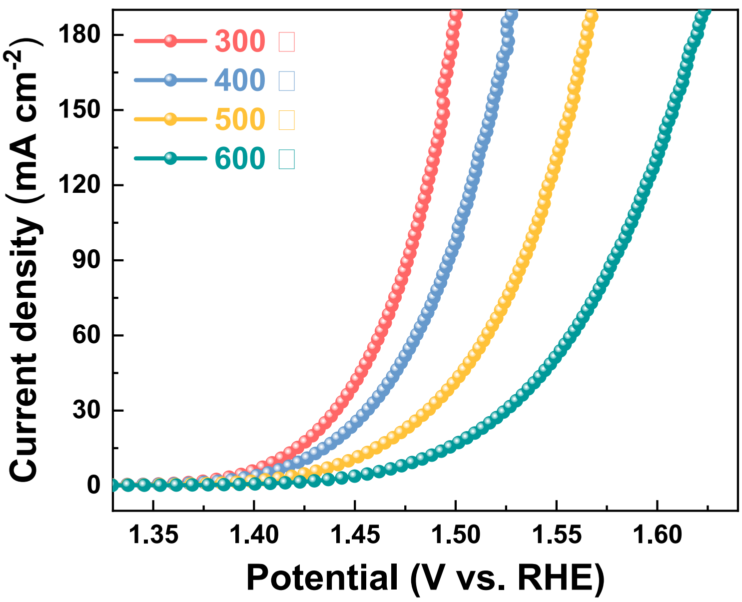

Figure S9. The LSV curves of 300 °C, 400 °C, 500 °C, and 600 °C.

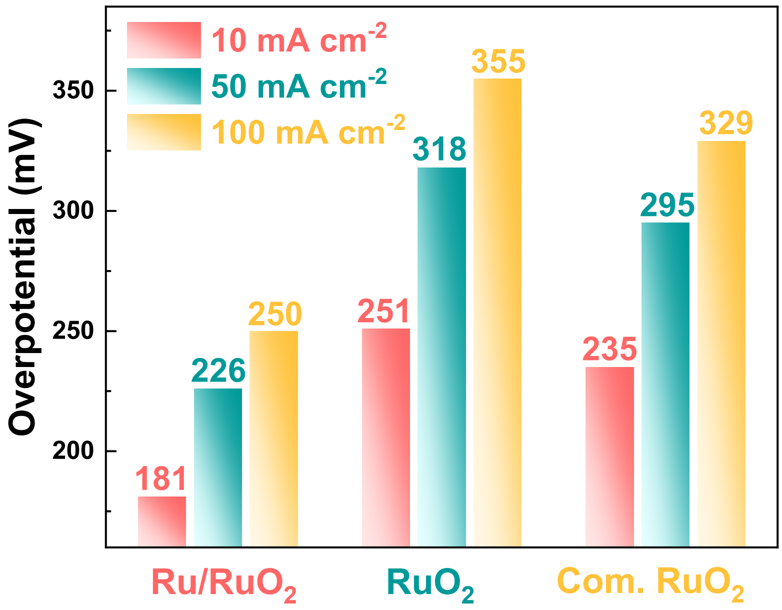

Figure S10. The overpotentials at current densities of 10, 50, 100 mA cm^{-2} of Ru/RuO_2, RuO_2, and Com. RuO_2.

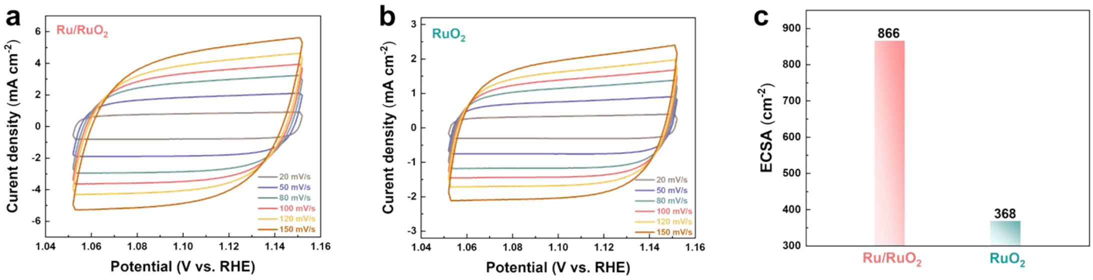

Figure S11. The CV curves of (a) Ru/RuO_2 and (b) RuO_2. (c) The ECSA of Ru/RuO_2 and RuO_2.

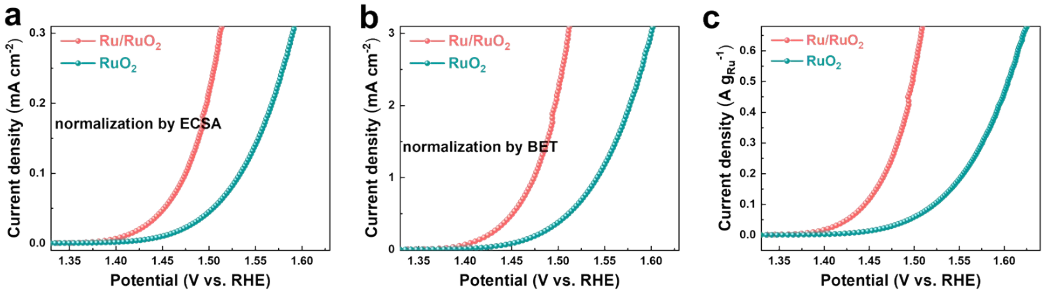

Figure S12. The specific OER activity normalized by (a) BET surface area, (b) ECSA, and (c) Ru mass loading for Ru/RuO_2 and RuO_2.

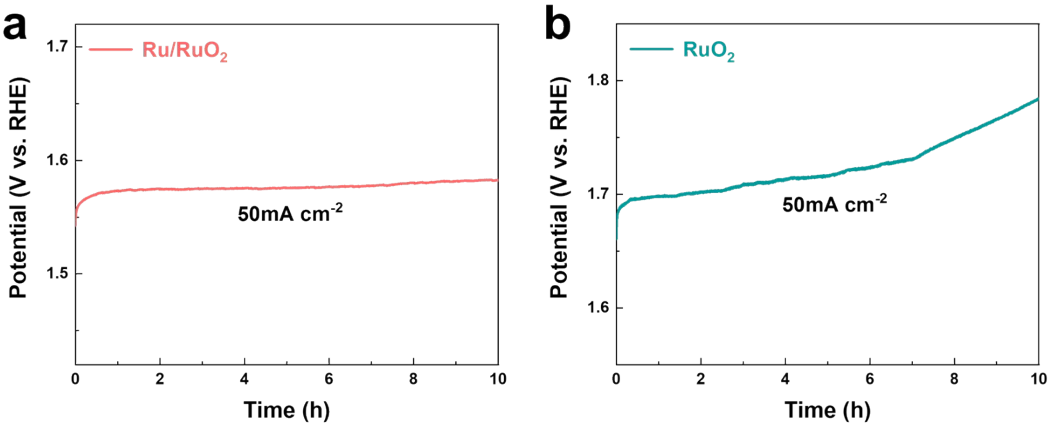

Figure S13. The chronopotentiometry curves for Ru/RuO_2 and RuO_2 at a current density of 50 mA cm^{-2}.

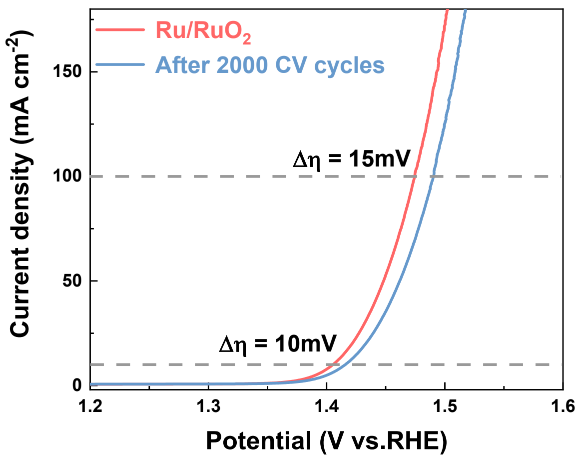

Figure S14. The LSV curves for Ru/RuO_2 and after 2000 CV cycles.

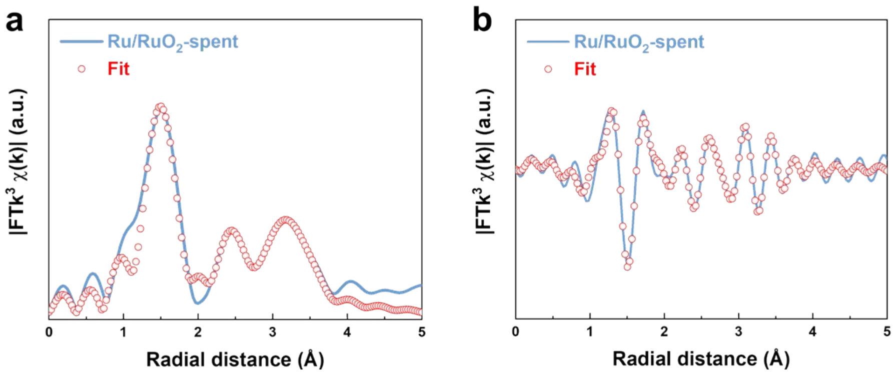

Figure S15. FT-EXAFS spectra of Ru/RuO_2-spent.

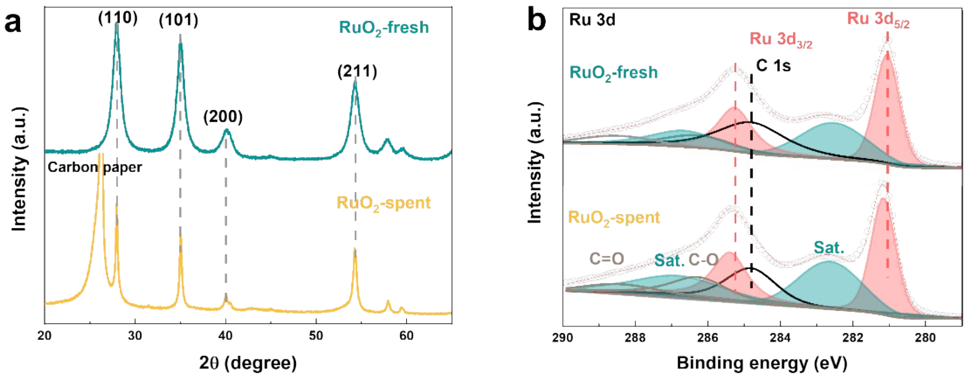

Figure S16. (a) The XRD and (b) XPS of RuO_2-fresh and RuO_2-spent.

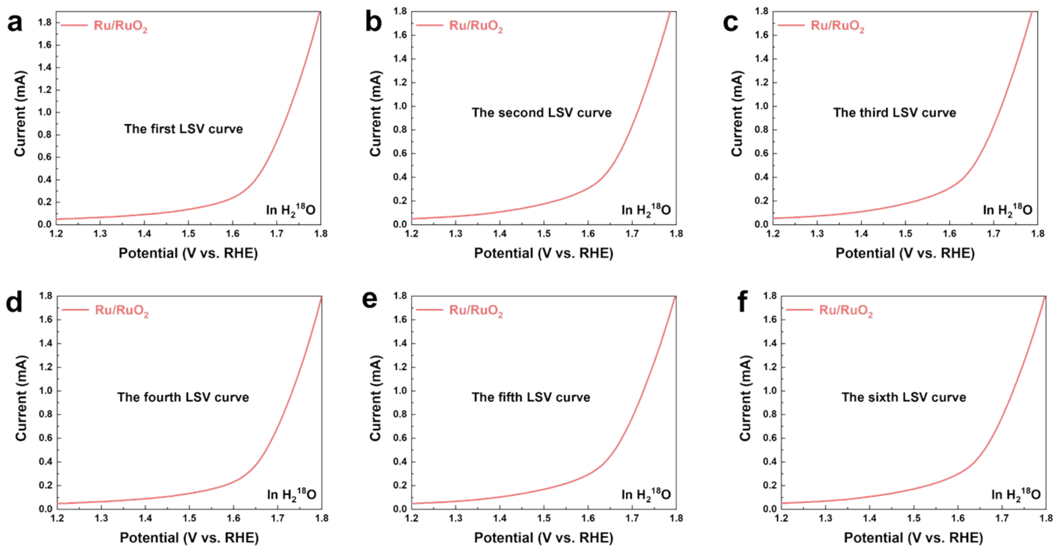

Figure S17. LSV curves of Ru/RuO_2 recorded during the DEMS measurements in $H_2{}^{18}O$.

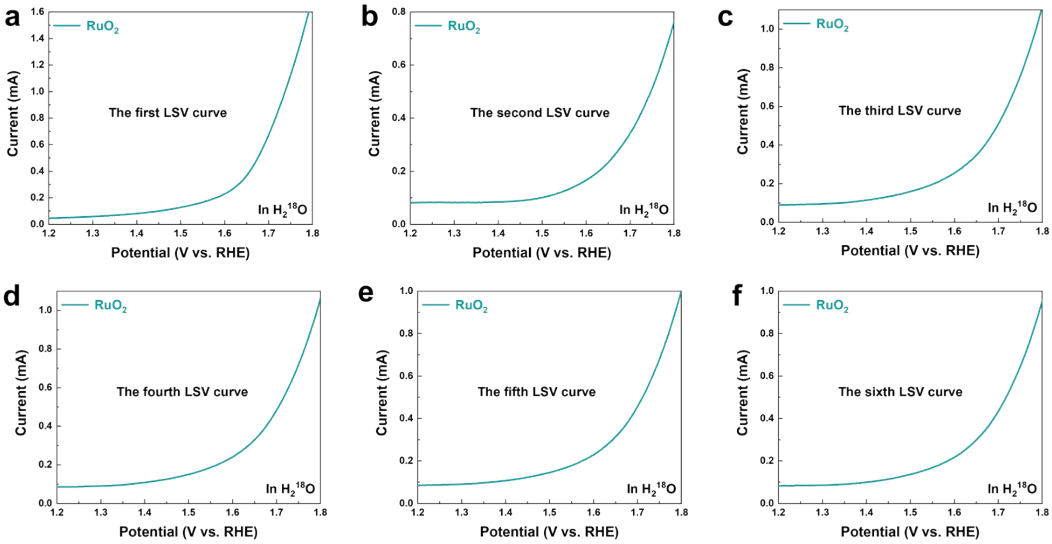

Figure S18. LSV curves of RuO_2 recorded during the DEMS measurements in $H_2^{18}O$.

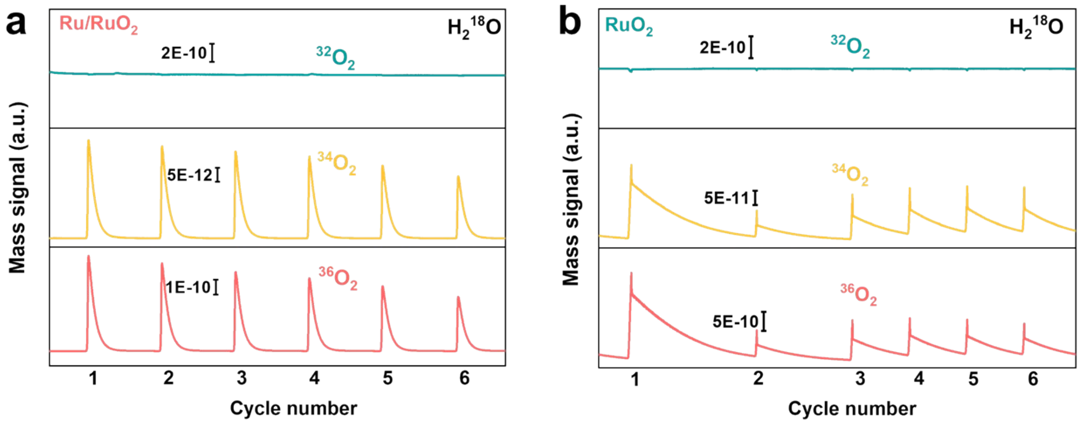

Figure S19. The operando DEMS results in $H_2{}^{18}O$ for (a) Ru/RuO_2 and (b) RuO_2.

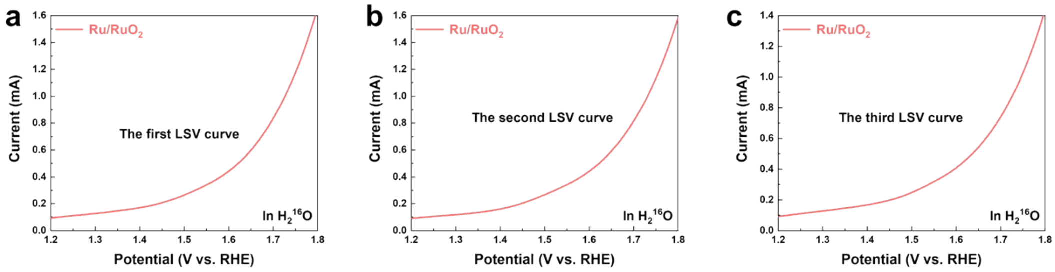

Figure S20. LSV curves of Ru/RuO_2 recorded during the DEMS measurements in $H_2{}^{16}O$.

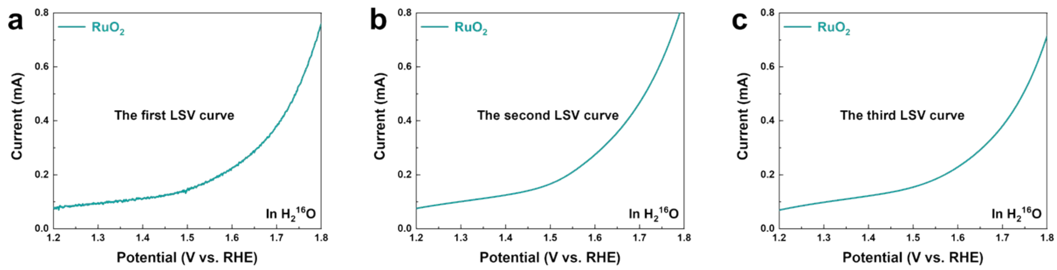

Figure S21. LSV curves of RuO_2 recorded during the DEMS measurements in $H_2{}^{16}O$.

a

b

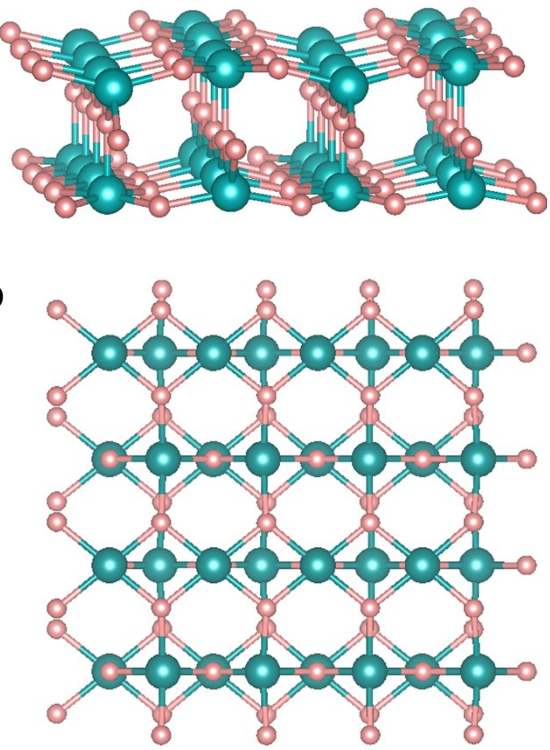

Figure S22. The (a) front, and (b) top views of optimized RuO_2 models. In these representations, Ru atoms are depicted in green, while O atoms are shown in red.

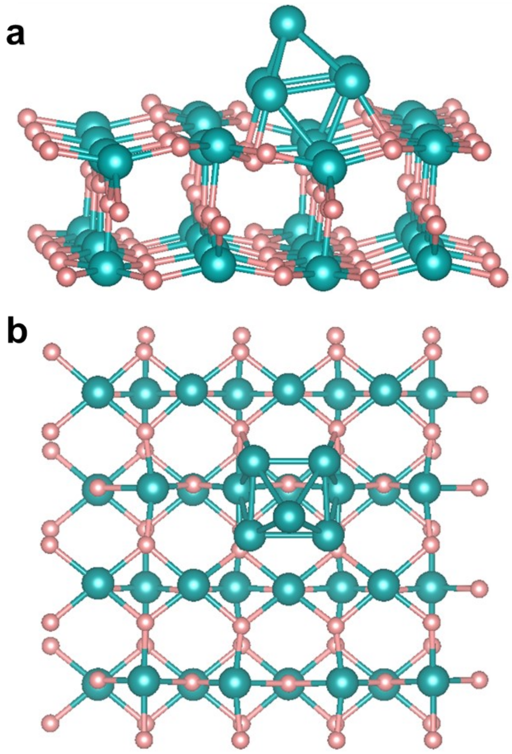

Figure S23. The (a) front, and (b) top views of optimized Ru/RuO_2 models.

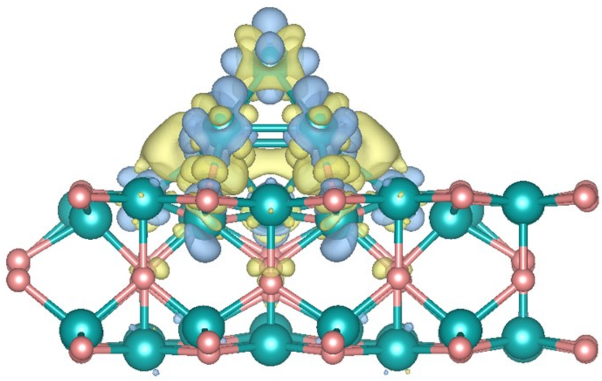

Figure S24. Front view differential charge density of Ru/RuO_2 (yellow and blue contours represent the charge accumulation and depletion, respectively) (green: Ru, red: O).

Table S1. Ru K-edge EXAFS fitted parameters of Ru foil, RuO_2, and Ru/RuO_2.

Catalyst	Shell	CN	R (Å)	$\sigma^2(10^{-3}Å^2)$	ΔE_0 (eV)	R-factor
Ru foil	Ru-Ru	12.0	2.67	3.8	5.3	0.024
RuO_2	Ru-O	6.3	1.97	2.2	1.0	0.026
	Ru-O-Ru	3.4	3.18	2.2	4.0	0.026
	Ru-O-Ru	5.1	3.62	2.2	10.0	0.026
Ru/RuO_2	Ru-O	5.6	1.98	4.0	1.0	0.014
	Ru-Ru	2.1	2.71	4.0	3.0	0.014
	Ru-O-Ru	2.4	3.20	4.0	6.0	0.014
	Ru-O-Ru	2.6	3.61	4.0	9.0	0.014

CN, coordination numbers; R, the internal atomic distance; σ^2, the Debye-Waller factor; ΔE_0, inner potential correction to account for the difference in the inner potential between the sample and the reference compound. R-factor indicates the goodness of the fit. EXAFS data fitting analysis range: in R-space (1.0-4.0 Å) and in the k-space (3.0-11.0 $Å^{-1}$). $S_0^2 = 0.78$

Table S2. The Ru content in Ru/RuO_2, and RuO_2 measured by STEM EDS mapping and ICP-OES analysis.

Catalyst	EDS analysis (at. %)		Content of Ru based on ICP-OES
	Ru	O	
Ru	72.83	27.18	/
Ru/RuO_2	34.38	65.62	0.85
RuO_2	22.26	77.74	0.71

Table S3. Comparison of OER performances in acidic media for Ru/RuO_2 with reported representative RuO_2-based OER electrocatalysts.

Catalyst	Overpotential (mV)	Tafel slope (mV dec^{-1})	Stability (h)	References
Ru/RuO_2	181	52.2	260	This work
RuO_2@COF-O (3)	218	64.3	42	[4]
PdO@RuO_2	189	65.2	102.9	[5]
RuO_2-O_v	198	57.1	100	[6]
Ga-RuO_2	217.5	60.5	150	[7]
Co-RuO_2/TiO_2	266	65	50	[8]
$La_{0.1}Ru_{0.9}O_2$	188	76.6	63	[9]
Ru/$ZnRuO_2$	184	52.5	30	[10]
$Mn_{0.4}Ru_{0.6}O_2$	196	58.4	120	[11]
RuO_2/$MnO_{2-\gamma}$	220	72.2	80	[12]
SS Pt-RuO_2 HNSs	228	51	100	[13]
a/c-RuO_2	205	48.6	60	[14]
$Mn_{0.73}Ru_{0.27}O_{2-\delta}$	208	65.3	10	[15]
$Y_{1.7}Sr_{0.3}Ru_2O_7$	264	44.8	28	[16]
Ni-Ru@RuO_x-HL	184	44	30	[17]

Table S4. Ru K-edge EXAFS fitted parameters of Ru/RuO_2-fresh, and Ru/RuO_2-spent.

Catalyst	Shell	CN	R (Å)	σ^2(10^{-3}Å^2)	ΔE_0 (eV)	R-factor
fresh	Ru-O	5.6	1.98	4.0	1.0	0.014
	Ru-Ru	2.1	2.71	4.0	3.0	0.014
	Ru-O-Ru	2.4	3.20	4.0	6.0	0.014
	Ru-O-Ru	2.6	3.61	4.0	9.0	0.014
spent	Ru-O	5.7	2.00	4.0	3.5	0.037
	Ru-Ru	2.1	2.73	4.0	5.0	0.037
	Ru-O-Ru	2.5	3.21	4.0	7.0	0.037
	Ru-O-Ru	2.8	3.61	4.0	9.0	0.037

CN, coordination numbers; R, the internal atomic distance; σ^2, the Debye-Waller factor; ΔE_0, inner potential correction to account for the difference in the inner potential between the sample and the reference compound. R-factor indicates the goodness of the fit. EXAFS data fitting analysis range: in R-space (1.0-4.0 Å) and in the k-space (3.0-11.0 Å^{-1}). S_0^2 = 0.78

Table S5. The CONTCAR of RuO_2.

RuO_2

1.00000000000000

12.4454002379999995	0.0000000000000000	0.0000000000000000
0.0000000000000000	12.6784000396999996	0.0000000000000000
0.0000000000000000	0.0000000000000000	23.1695995331000013

Ru O

32 48

Direct

0.1759228476414236	0.3260592728931186	0.2242042459976616
0.1840622163460637	0.0760026109987706	0.3506157794121307
0.0558597734372626	0.0759914610219781	0.2102893355311650
0.0558753548806266	0.3259979798287276	0.3635837192898705
0.4206853888053104	0.3260418581636202	0.2280304863910061
0.4228742812316924	0.0759950677094139	0.3485897096230275
0.3050367449348386	0.0759841272883364	0.2112213129747573
0.3054273598593511	0.3260407300011181	0.3638238685133572
0.6871821259870643	0.3259650688093103	0.2281130755866840
0.6799295579119828	0.0759946837664529	0.3465037505712871
0.5547732657026643	0.0759787918925525	0.2162601160235269
0.5553621457679867	0.3258928526291314	0.3570043932837450
0.9371396521815143	0.3259197926371655	0.2244686921835068
0.9402741120725722	0.0760165765075058	0.3469131421193197
0.8061192751204516	0.0759911914639346	0.2155909958988076
0.8069518566287712	0.3260703579531636	0.3604106669341931

0.1758511222587131	0.8259212488052512	0.2242313886053680
0.1844645670712879	0.5760178091991790	0.3505185073386130
0.0558933964234782	0.5759843438611512	0.2102334915725947
0.0558892056998062	0.8260087982112978	0.3635964670113907
0.4206631041610365	0.8259304692206442	0.2280898018496771
0.4236475745325166	0.5760358272029293	0.3488503936901424
0.3052635497824738	0.5759913032128736	0.2112921084354156
0.3054441710218541	0.8259945047513710	0.3638844701751083
0.6872434943320798	0.8260113485411722	0.2281264301412733
0.6787065451518970	0.5760055866599600	0.3465716864929291
0.5549973560096575	0.5759894978702746	0.2158349780384725
0.5554339458848077	0.8261246602456040	0.3570171312981500
0.9371660279035012	0.8260594282271256	0.2244508636327893
0.9407435920026543	0.5759642695877147	0.3468235732219469
0.8062611999352356	0.5759800122176699	0.2160293636958457
0.8070501245316208	0.8259179774729688	0.3603948138362583
0.1816495563887486	0.1766283118725411	0.2047322745911444
0.1797242911507482	0.4263172119056478	0.3695697414796584
0.1818144876380998	0.4754921935555600	0.2047520247559049
0.1798453274311669	0.2257901037617032	0.3695528463490874
0.0563707040136521	0.3258468751932497	0.2808773505468736
0.0565722420734289	0.0759855693796467	0.2927612488902938
0.4323310407240939	0.1774531499386995	0.2087065010656133
0.4326212570989156	0.4259437518888305	0.3648872219527348
0.4324815061185490	0.4745429592609653	0.2083770271409833

0.4324754754578777	0.2259009729987440	0.3647579994739658
0.3042985181386868	0.3264018426879289	0.2812568746228621
0.3045347799464366	0.0759354355907860	0.2937570559955773
0.6795665755295346	0.1764611710741733	0.2116410945187042
0.6809663304359930	0.4263398707032238	0.3633472800606299
0.6798166627262034	0.4754780277174362	0.2115734896930164
0.6810352554533026	0.2256081471062785	0.3633253663675617
0.5548705749867295	0.3259740581561630	0.2742749757662821
0.5538745062398220	0.0759909139467041	0.2985958839490550
0.9289586134141956	0.1756435232143261	0.2079673101565120
0.9292658777902645	0.4280110323548527	0.3673159292198918
0.9289889963098901	0.4763074238095371	0.2083426994421629
0.9292451029417919	0.2241344431049512	0.3672387221553137
0.8086260438433115	0.3260106949512789	0.2780470475266341
0.8075797079271609	0.0760493924744239	0.2983732059093498
0.1818111379947212	0.6765014356076620	0.2047710444988056
0.1798293646862348	0.9262410802427112	0.3696302153551656
0.1816474891168696	0.9753481268909354	0.2047282339209602
0.1797278524916521	0.7257103078459366	0.3696186802544759
0.0563770741772558	0.8261800040008538	0.2808898009579366
0.0567493687599807	0.5760014657865398	0.2927501078824264
0.4324916992855137	0.6774727732776498	0.2084112516126666
0.4325263160877526	0.9261071723655050	0.3648025142342348
0.4323348827106912	0.9744830382291099	0.2087110765334046
0.4326639983728668	0.7261150742224558	0.3649223690871324

0.3043080036196741	0.8256540442854217	0.2813326195126109
0.3048663501988074	0.5760938229037080	0.2938073986183269
0.6798051106698111	0.6764972814860073	0.2116049016282773
0.6811298568461694	0.9263915423330786	0.3633034606731300
0.6795578354297334	0.9755271552456293	0.2116518325511478
0.6810470507978437	0.7256695035541227	0.3633146996435670
0.5548817538047572	0.8260503916613047	0.2742933837569907
0.5537913612789964	0.5760062753340875	0.2981651377293844
0.9289911519241940	0.6756425372696455	0.2083468049036057
0.9292946758921445	0.9278942842009172	0.3672482062619054
0.9289634006562935	0.9763795312235999	0.2079589933395241
0.9293226378681254	0.7239328043107633	0.3672950314583048
0.8086801699273636	0.8260453111206090	0.2780323213398717
0.8074938044118483	0.5759279871026735	0.2988102552463445

Table S6. The CONTCAR of Ru/RuO_2.

Ru/RuO_2

1.00000000000000

12.4454002379999995	0.0000000000000000	0.0000000000000000
0.0000000000000000	12.6784000396999996	0.0000000000000000
0.0000000000000000	0.0000000000000000	23.1695995331000013

Ru O

37 48

Direct

0.1814989041543615	0.3247641222032565	0.2241791980008501
0.1766543271053942	0.0834195780907261	0.3548348000850621
0.0563516532493661	0.0745259888585678	0.2155620430983824
0.0562416545512147	0.3353056694969879	0.3615612234299775
0.4159392308174235	0.3248301754475587	0.2279619902974067
0.4151619103846005	0.0786420769054557	0.3488699376035138
0.3059279610748327	0.0742522057437462	0.2122185083627423
0.3071277095244654	0.3302956479263467	0.3688216750421857
0.6966012159074363	0.3248689443462671	0.2278294726688095
0.6971827843380823	0.0785029424907749	0.3487772259338548
0.5563591454153971	0.0755908603426635	0.2239577685005153
0.5563481895137807	0.3199088401386007	0.3523663813429192
0.9309947327351549	0.3247434332201738	0.2240459688597905
0.9356952391409805	0.0832598232373962	0.3548394972619987
0.8067380485389695	0.0741302217248621	0.2122530079827136
0.8055248264150552	0.3302501722445939	0.3687398977154887

0.1800583685404017	0.8242442317779615	0.2270271882379352
0.1996699746415420	0.5806880764322141	0.3470128755469705
0.0563690904788011	0.5759305031418276	0.2193145340957737
0.0563019722473361	0.8275655948199641	0.3629279719461566
0.4225626175813188	0.8234729491505570	0.2305473669848444
0.4257789502823006	0.5798080297677296	0.3464426248199620
0.3058598372719278	0.5764474447703436	0.2068446355352450
0.3021016409520195	0.8334534648035822	0.3668923062819186
0.6899304120843098	0.8233592015856019	0.2304974784661474
0.6868463570722477	0.5797629611799607	0.3461073663024531
0.5562640092926221	0.5754633609431909	0.2120587248587986
0.5562220505325854	0.8349278714675186	0.3604682574344141
0.9323116739502382	0.8242089762619638	0.2270167577433089
0.9131966253512573	0.5807372179234691	0.3468825963801632
0.8068288817013540	0.5764637986517007	0.2066941412448643
0.8101724324611485	0.8332581567749611	0.3668602439491091
0.4544490512608864	0.4590743671273619	0.4263736506831276
0.4650628721335457	0.6498178941568977	0.4424827260931807
0.6599202552920610	0.4587461128827115	0.4262017468771294
0.6498350048511781	0.6495379518748883	0.4423340796031291
0.5579200982393411	0.5064641662730430	0.5109493305074341
0.1806251645109380	0.1739294155621030	0.2045791640898775
0.1828836163934733	0.4346430044092754	0.3658867244185966
0.1809950596060219	0.4752413375367310	0.2098342264543523
0.1806338255516899	0.2345949743529495	0.3740568088250503

0.0563529642488905	0.3203551748119980	0.2803191990124989
0.0562355975242703	0.0856859934011085	0.2975806258952778
0.4329525333837945	0.1748268459270225	0.2107227544663509
0.4286750890039740	0.4216135891636033	0.3420875842187446
0.4319271451752537	0.4733277243358422	0.2074060926682671
0.4324968230429919	0.2253838268590296	0.3660971262891035
0.3005396240063763	0.3152171400348606	0.2797637761417911
0.3027826956371690	0.0802961326630497	0.2945276126407748
0.6797329371227953	0.1748328521707076	0.2106818978487162
0.6840675552282922	0.4215381070319806	0.3417411100815915
0.6806653609616425	0.4733459143684657	0.2073767059051191
0.6802246639316690	0.2253011232113327	0.3659346736708942
0.5563006995533323	0.3158446283749385	0.2681989855253034
0.5561798180110531	0.0769225803210421	0.3059686219568565
0.9320742374562241	0.1738016537797198	0.2044678842438012
0.9296532171166363	0.4345917207704597	0.3657130734187378
0.9317608627396322	0.4752999731476772	0.2097946313061953
0.9318162238393813	0.2345182613483646	0.3740274104384253
0.8120927717510342	0.3149780789265337	0.2795612063185529
0.8098776541465823	0.0801518895508344	0.2945916571621780
0.1793618013836613	0.6765753247821263	0.2060909394295687
0.1772401131091336	0.9314575442781798	0.3687667039895834
0.1816516607388472	0.9738270298994985	0.2082858393618235
0.1805055410254439	0.7261444910176610	0.3706471129019130
0.0563239000657543	0.8203979219498894	0.2809210486238680

0.0563508642682778	0.5814731549463181	0.3014812310357820
0.4335279893902827	0.6786473347185190	0.2034674500170952
0.4301795667158964	0.9309945307330436	0.3656435455303540
0.4332010161870590	0.9731766489218362	0.2140244418560975
0.4293748045407945	0.7335622180533768	0.3683015386484262
0.3034379411494417	0.8247833260437182	0.2829579099209885
0.3065382779868129	0.5900458980339575	0.2887857330994567
0.6790372282735802	0.6785401653183546	0.2035195388961877
0.6823348778761618	0.9308873562704206	0.3654755927853757
0.6794560444952940	0.9731410287377167	0.2142382524675684
0.6830101272694210	0.7334137456818807	0.3678301489411380
0.5561677191289850	0.8222977850959041	0.2773471043175235
0.5560814464654799	0.5910421011923718	0.2931403863938814
0.9334300123740488	0.6765074071146575	0.2060393219148773
0.9351317798456908	0.9312276004952869	0.3688417292840501
0.9311251087612593	0.9738514555721111	0.2082710342770350
0.9319650328150909	0.7263082447216448	0.3705160596230523
0.8089430408617244	0.8247556793797829	0.2829111093295295
0.8062090182438941	0.5901764847967346	0.2886517565795628

Table S7. The Bader charge results of RuO_2.

RuO_2	X	Y	Z	CHARGE	MIN DIST	ATOMIC VOL
1	2.189432	4.133906	5.194717	12.855816	0.946214	46.748569
2	2.290725	0.963596	8.123632	12.868524	0.947245	47.809930
3	0.695200	0.963444	4.872312	12.572696	0.950979	56.799416
4	0.695387	4.133133	8.424096	12.551381	0.950879	55.635444
5	5.235593	4.133691	5.283364	12.729832	0.938061	45.530648
6	5.262836	0.963495	8.076691	12.781944	0.934331	51.641410
7	3.796307	0.963356	4.893906	12.554100	0.949342	56.436931
8	3.801161	4.133678	8.429657	12.563611	0.952385	60.022641
9	8.552255	4.132715	5.285287	12.724340	0.916319	51.797265
10	8.462001	0.963495	8.028359	12.713377	0.929817	50.700995
11	6.904372	0.963292	5.010658	12.557685	0.946669	49.692877
12	6.911702	4.131802	8.271640	12.528590	0.952760	43.367727
13	11.663082	4.132144	5.200857	12.819639	0.941389	52.082528
14	11.702086	0.963774	8.037835	12.740768	0.938508	42.950587
15	10.032473	0.963444	4.995157	12.548535	0.942351	49.080391
16	10.042840	4.134046	8.350579	12.539952	0.940569	54.503560
17	2.188536	10.471357	5.195343	12.855476	0.948053	46.805339
18	2.295741	7.302987	8.121385	12.866253	0.947430	47.894205
19	0.695611	7.302556	4.871015	12.574597	0.950716	58.016632
20	0.695561	10.472473	8.424374	12.551025	0.950664	55.723245
21	5.235319	10.471471	5.284754	12.728905	0.936931	45.492213
22	5.272469	7.303215	8.082715	12.786002	0.939531	53.323369
23	3.799133	7.302644	4.895551	12.552948	0.951271	54.949614

24	3.801373	10.472295	8.431047	12.563809	0.952986	59.967280
25	8.553014	10.472498	5.285588	12.723717	0.915557	51.811722
26	8.446780	7.302834	8.029935	12.714650	0.941553	50.327226
27	6.907160	7.302619	5.000811	12.546872	0.936700	50.521163
28	6.912598	10.473943	8.271941	12.525998	0.951386	43.342339
29	11.663406	10.473106	5.200440	12.820295	0.940562	52.223925
30	11.707935	7.302302	8.035773	12.731395	0.932892	42.686481
31	10.034241	7.302505	5.005306	12.559683	0.947283	48.199214
32	10.044060	10.471319	8.350208	12.538968	0.941031	54.486988
33	2.260707	2.239360	4.743559	6.929498	0.860778	61.912287
34	2.236737	5.405017	8.562789	6.925716	0.864295	62.307212
35	2.262748	6.028478	4.744022	6.920696	0.844237	62.545931
36	2.238243	2.862656	8.562395	6.917258	0.853647	62.331895
37	0.701560	4.131219	6.507808	6.828701	0.837182	11.895007
38	0.704061	0.963381	6.783155	6.803243	0.826567	10.745845
39	5.380532	2.249820	4.835658	6.938256	0.849577	58.647102
40	5.384141	5.400288	8.454286	6.931705	0.868690	54.023303
41	5.382411	6.016446	4.828012	6.932807	0.841399	59.123833
42	5.382324	2.864063	8.451297	6.926948	0.844822	56.479950
43	3.787123	4.138255	6.516612	6.807285	0.812101	10.637593
44	3.790060	0.962734	6.806232	6.818936	0.809963	11.168627
45	8.457483	2.237243	4.903637	6.939411	0.862439	52.788104
46	8.474894	5.405309	8.418605	6.938054	0.864181	54.479230
47	8.460594	6.028300	4.902062	6.927350	0.840457	53.750029
48	8.475753	2.860348	8.418095	6.928687	0.851664	54.998627

49	6.905592	4.132829	6.354842	6.816092	0.840833	10.768412
50	6.893196	0.963444	6.918350	6.785409	0.814614	10.451062
51	11.561266	2.226885	4.818512	6.929025	0.864424	56.587496
52	11.565087	5.426495	8.510565	6.939896	0.843384	59.337516
53	11.561640	6.038811	4.827224	6.923045	0.845354	56.323390
54	11.564826	2.841661	8.508781	6.933417	0.840157	60.362206
55	10.063674	4.133298	6.442238	6.806001	0.818979	10.327647
56	10.050656	0.964180	6.913183	6.800315	0.820842	10.430610
57	2.262711	8.576950	4.744462	6.928583	0.862304	61.687321
58	2.238044	11.743254	8.564179	6.925951	0.865328	62.045222
59	2.260670	12.365852	4.743466	6.920739	0.852917	62.543110
60	2.236787	9.200842	8.563924	6.917664	0.853055	62.214123
61	0.701634	10.474641	6.508109	6.829616	0.837220	11.888660
62	0.706264	7.302771	6.782900	6.805193	0.828256	10.750429
63	5.382536	8.589274	4.828800	6.937837	0.849449	59.383003
64	5.382959	11.741555	8.452340	6.931812	0.866677	54.738753
65	5.380582	12.354885	4.835750	6.934075	0.838366	58.997245
66	5.384677	9.205976	8.455097	6.926913	0.848326	56.131922
67	3.787235	10.467972	6.518373	6.807527	0.813538	10.643940
68	3.794179	7.303950	6.807391	6.824020	0.828250	10.783574
69	8.460445	8.576900	4.902803	6.941087	0.862084	52.673153
70	8.476935	11.745168	8.417585	6.939522	0.863432	54.437622
71	8.457371	12.368122	4.903892	6.927090	0.841139	53.727109
72	8.475902	9.200335	8.417863	6.928638	0.852350	55.234525
73	6.905728	10.472992	6.355259	6.816641	0.841162	10.855155

74	6.892151	7.302834	6.908364	6.795832	0.801882	10.425321
75	11.561665	8.566072	4.827317	6.929207	0.862979	56.414716
76	11.565448	11.764211	8.508989	6.939539	0.844802	58.989488
77	11.561316	12.378936	4.818327	6.922748	0.846481	57.087500
78	11.565796	9.178312	8.510078	6.934701	0.838070	60.392883
79	10.064346	10.472929	6.441890	6.806719	0.819376	10.321653
80	10.049586	7.301846	6.923308	6.789214	0.837850	10.518058

Table S8. The Bader charge results of Ru/RuO_2.

Ru/RuO_2	X	Y	Z	CHARGE	MIN DIST	ATOMIC VOL
1	2.258828	4.117488	5.194138	12.833623	0.954335	48.952393
2	2.198530	1.057632	8.221385	12.870661	0.967860	46.717186
3	0.701323	0.944870	4.994485	12.526351	0.943229	39.805290
4	0.699954	4.251144	8.377224	12.540286	0.934391	29.213183
5	5.176527	4.118325	5.281788	12.705858	0.898115	47.701326
6	5.166857	0.997055	8.083178	12.700715	0.918602	35.682905
7	3.807396	0.941397	4.917029	12.552696	0.948136	60.678498
8	3.822331	4.187625	8.545458	12.763484	0.937826	31.989296
9	8.669478	4.118819	5.278707	12.703746	0.901682	47.720720
10	8.676721	0.995292	8.081024	12.719408	0.905913	35.760832
11	6.924110	0.958373	5.189017	12.494127	0.951013	30.759386
12	6.923973	4.055934	8.164179	12.687197	0.925426	14.804407
13	11.586605	4.117222	5.191056	12.822949	0.945311	50.486254
14	11.645099	1.055604	8.221478	12.902187	0.972055	48.026787
15	10.040177	0.939850	4.917817	12.554057	0.943957	60.863267
16	10.025081	4.187042	8.543558	12.771003	0.939115	31.628222
17	2.240894	10.450095	5.260125	12.808758	0.942893	44.558849
18	2.484973	7.362195	8.040152	12.724255	0.912128	22.904253
19	0.701535	7.301884	5.081441	12.544352	0.950553	28.066842
20	0.700701	10.492213	8.408897	12.521702	0.946756	35.649054
21	5.258966	10.440320	5.341682	12.730535	0.926724	41.035552
22	5.298990	7.351038	8.026946	12.985476	0.973075	13.975769
23	3.806550	7.308426	4.792516	12.616223	0.940805	71.528364

24	3.759780	10.566851	8.500741	12.625287	0.956716	34.106730
25	8.586455	10.438875	5.340523	12.737813	0.950859	41.151562
26	8.548073	7.350467	8.019161	12.990824	0.963850	13.936277
27	6.922928	7.295950	4.913322	12.529573	0.951821	45.293693
28	6.922405	10.585551	8.351899	12.622384	0.931053	19.974401
29	11.602996	10.449651	5.259893	12.808646	0.942097	45.870918
30	11.365102	7.362816	8.037140	12.716534	0.919874	22.882038
31	10.041310	7.308641	4.789017	12.602812	0.931262	72.652843
32	10.082915	10.564378	8.499999	12.635723	0.947752	34.092978
33	5.655800	5.820324	9.878915	13.780329	0.987756	65.342495
34	5.787895	8.238653	10.252154	13.774721	0.981909	144.646655
35	8.212968	5.816165	9.874930	13.748933	0.986043	64.048762
36	8.087457	8.235103	10.248702	13.729764	0.983659	143.137829
37	6.943538	6.421153	11.838484	14.170688	1.121198	652.753576
38	2.247950	2.205141	4.740014	6.916623	0.863095	63.797350
39	2.276065	5.510578	8.477455	6.914419	0.828663	19.560082
40	2.252555	6.025295	4.861770	6.918571	0.860089	41.024974
41	2.248062	2.974289	8.666751	6.912117	0.853598	35.222394
42	0.701336	4.061589	6.494879	6.793284	0.818429	10.911925
43	0.699880	1.086361	6.894833	6.801692	0.845906	10.927440
44	5.388273	2.216527	4.882368	6.927063	0.854743	50.862843
45	5.335032	5.345391	7.926042	6.910070	0.855075	9.112547
46	5.375504	6.001042	4.805514	6.938790	0.852863	44.889599
47	5.382598	2.857509	8.482321	6.915113	0.829049	17.942299
48	3.740341	3.996447	6.482020	6.774881	0.771828	10.414742

49	3.768256	1.018025	6.824096	6.816646	0.813200	10.570244
50	8.459549	2.216603	4.881418	6.922445	0.853238	47.647376
51	8.513500	5.344427	7.918002	6.908318	0.848738	9.104437
52	8.471148	6.001270	4.804842	6.939294	0.849369	43.492199
53	8.465672	2.856456	8.478568	6.907925	0.828457	17.842510
54	6.923388	4.004409	6.214064	6.829152	0.842329	10.996199
55	6.921883	0.975261	7.089179	6.821455	0.862452	10.887948
56	11.600034	2.203531	4.737442	6.917834	0.864882	67.724388
57	11.569903	5.509931	8.473424	6.910623	0.829600	19.427853
58	11.596138	6.026044	4.860866	6.924493	0.860820	42.570471
59	11.596823	2.973313	8.666056	6.912228	0.861897	36.153994
60	10.106822	3.993417	6.477317	6.784509	0.782172	10.478213
61	10.079256	1.016199	6.825579	6.796965	0.776798	10.499017
62	2.232232	8.577888	4.775046	6.920817	0.842959	53.470408
63	2.205823	11.809397	8.544184	6.913631	0.866724	34.958640
64	2.260732	12.346568	4.825903	6.931271	0.863219	54.056449
65	2.246469	9.206344	8.587743	6.927105	0.833426	23.384158
66	0.700975	10.401334	6.508827	6.811490	0.838266	10.860091
67	0.701311	7.372147	6.985194	6.794568	0.831163	11.278641
68	5.395429	8.604158	4.714249	6.923399	0.839750	57.853020
69	5.353762	11.803527	8.471825	6.926711	0.833899	19.975459
70	5.391360	12.338327	4.958850	6.928933	0.858060	45.577545
71	5.343744	9.300392	8.533410	6.962977	0.879254	10.593869
72	3.776407	10.456929	6.556024	6.800208	0.797130	10.440836
73	3.814988	7.480839	6.691056	6.815961	0.788499	10.364672

74	8.450887	8.602802	4.715477	6.937109	0.842725	55.018374
75	8.491932	11.802158	8.467933	6.917063	0.831877	19.868265
76	8.456102	12.337871	4.963809	6.931481	0.857732	42.351852
77	8.500333	9.298516	8.522474	6.958658	0.878215	10.519821
78	6.921733	10.425423	6.426019	6.805358	0.840537	10.974690
79	6.920650	7.493467	6.791937	6.818826	0.855187	10.680259
80	11.616910	8.577026	4.773841	6.906433	0.843957	55.073381
81	11.638092	11.806481	8.545922	6.926013	0.870249	36.861686
82	11.588223	12.346873	4.825556	6.930477	0.861054	56.729599
83	11.598677	9.208423	8.584708	6.923069	0.835950	23.770267
84	10.067619	10.456586	6.554935	6.796581	0.807943	10.426379
85	10.033593	7.482487	6.687951	6.823666	0.801071	10.330468

Table S9. Band center of Ru and O for Ru/RuO_2 and RuO_2.

	Ru d band center	O p band center
Ru/RuO_2	-1.236	-3.929
RuO_2	-1.175	-3.928

Table S10. Comparison of PEMWE performances for Ru/RuO_2 with reported representative RuO_2-based OER electrocatalysts.

Catalyst	Potential @ 1A cm^{-2} (V)	Stability (h)	References
Ru/RuO_2	1.67	120 @ 1Acm^{-2}	This work
$22RuO_2/MnCo_2O_{4.5}$	1.83	130 @ 1Acm^{-2}	[18]
$Mg_{0.23}Ir_{0.13}Ru_{0.64}O_2$	1.72	42 @ 0.5Acm^{-2}	[19]
C,Ta-RuO_2	1.63	100 @ 1Acm^{-2}	[20]
Na/Hf-RuO_2	1.65	85 @ 0.5Acm^{-2}	[21]
La-RuO_2@TM	1.81	120 @ 1Acm^{-2}	[22]
LD-B/RuO_2	1.63	300 @ 0.25Acm^{-2}	[23]
Co_3O_4/Ni-RuO_2/rGO	1.97	100 @ 0.5Acm^{-2}	[24]
Zn-0.67RuO_2@ZnO	1.68	100 @ 1Acm^{-2}	[25]
Co-Ru@RuO_2	1.65	70 @ 1Acm^{-2}	[26]
RuFe@CF	1.90	250 @ 0.2Acm^{-2}	[27]

References

1. B. Ravel and M. Newville, *J. Synchrotron Radiat.,* 2005, **12**, 537-541.
2. S. Grimme, *J. Comput. Chem.,* 2006, **27**, 1787-1799.
3. J. Nørskov, J. Rossmeisl, A. Logadottir, L. Lindqvist, J. Kitchin, T. Bligaard and H. Jonsson, *J. Phys. Chem. B,* 2004, **108**, 17886-17892.
4. K. Wang, S. Xu, D. Wang, Z. Kou, Y. Fu, M. Bielejewski, V. Montes-García, A. Ciesielski, Y. Hou and P. Samorì, *Adv. Mater.,* 2025, **37**, 2417374.
5. T. Gao, D. Jiao, L. Wang, X. Ge, X. Wen, L. Zhang, L. Zheng, X. Zou, W. Zhang, W. Zheng, J. Fan and X. Cui, *J. Am. Chem. Soc.,* 2025, **147**, 4159-4166.
6. X. Zou, Z. Li, Q. Liang, F. Liu, T. Xu, K. Song, Z. Jiang, W. Zhang and W. Zheng, *Nano Lett.,* 2024, **24**, 16151-16158.
7. L. Wu, W. Huang, D. Li, H. Jia, B. Zhao, J. Zhu, H. Zhou and W. Luo, *Angew. Chem. Int. Ed.,* 2025, **64**, e202413334.
8. L. Lu, Z. Xu, S. Wei, S. Zhao, X. Du, Y. Wang, L. Wu and G. Liu, *Chem. Eng. J.,* 2024, **500**, 157107.
9. C. Li, C. Yuan, X. Huang, H. Zhao, F. Wu, L. Xin, X. Zhang, S. Ye and Y. Chen, *eScience,* 2025, **5**, 100307.
10. X. Zhang, Z. Su, D. Xiang, W. Xu, Q. Guo, Y. Fan, X. Kang, Y. Sheng, F. Zheng and W. Chen, *Adv. Funct. Mater.,* 2024, **34**, 2409306.
11. L. Tan, X. Wu, H. Wang, J. Zeng, B. Mei, X. Pan, W. Hu, M, Faiza, Q. Xiao, Y. Zhao, C. Fu, C. Lin, X. Li and W. Luo, *ACS Catal.,* 2024, **14**, 11273-11285.
12. J. Li, M. Yao, Z. Yuan, J. Ma, S. Geng and F. Liu, *Chem. Eng. J.,* 2024, **496**, 153921.
13. J. Wang, H. Yang, F. Li, L. Li, J. Wu, S. Liu, T. Cheng, Y. Xu, Q. Shao and X. Huang, *Sci. Adv.,* 2022, **8**, eabl9271.
14. L. Zhang, H. Jang, H. Liu, M. Kim, D. Yang, S. Liu, X. Liu and J. Cho, *Angew. Chem. Int. Ed.,* 2021, **60**, 18821-18829.
15. K. Wang, Y. Wang, B. Yang, Z. Li, X. Qin, Q. Zhang, L. Lei, M. Qiu, G. Wu and Y. Hou, *Energy Environ. Sci.,* 2022, **15**, 2356-2365.
16. N. Zhang, C. Wang, J. Chen, C. Hu, J. Ma, X. Deng, B. Qiu, L. Cai, Y. Xiong and Y. Chai, *ACS Nano* 2021, **15**, 8537-8548.
17. A. Harzandi, S. Shadman, A. Nissimagoudar, D. Kim, H. Lim, J. Lee, M. Kim, H. Jeong, Y. Kim and K. Kim, *Adv. Energy Mater.,* 2021, **11**, 2003448.
18. D. Li, W. Ma, M. Eswaran, C. Li, J. Chen, G. Sun, S. Xi, S. Kozlov, C. He and L. Wang, *ACS Catal.*, 2025, **15**, 13069-1308.

19. Y. Lun, H. Chen, K. Wang, S. Song and Y. Wang, *Adv. Energy Mater.,* 2025, **15**, 2405657.
20. X. Jiang, J. Zhu, M. Jiang, P. Zhang, W. Wen, W. Cai, Y. Ding, P. Sun and M. Cao, *Adv. Mater.,* 2025, **37**, 2503354.
21. Y. Zhu, F. Wu, X. Zhang, Y. Lin, L. Zhang, T .Chan, Q. Zhang and L. Chen, *Adv. Mater.,* 2025, **37**, 2500449.
22. X. Zhang, H. Yin, C. Dang, H. Nie, Z. Huang, S. Zheng, M. Du, Z. Gu, J. Cao and X. Wu, *Angew. Chem.,* 2025, **137**, e202425569.
23. G. Chen, R. Lu, C. Ma, X. Zhang, Z. Wang, Y. Xiong and Y. Han, *Angew. Chem. Int. Ed.,* 2024, **63**, e202411603.
24. W. Yang, Z. Wang, J. Zhang, L. Jia, J. Li, X. Chen, X. Liu, H. Zhang, J. Lin, M. Zhao and Q. Chen, *Angew. Chem.,* 2025, **137**, e202509768.
25. Y. Qin, S. Deng, X. Zhou, Z. Yan, L. He, K. Li and T. Zhang, *J. Am. Chem. Soc.,* 2025, **147**, 30943-30955.
26. J. Chen, Y. Ma, C. Cheng, T. Huang, R. Luo, J. Xu, X. Wang, T. Jiang, H. Liu, S. Liu, T. Huang, L. Zhang and W. Chen, *J. Am. Chem. Soc.* 2025, **147**, 8720-8731.
27. J. Chen, Y. Ma, T. Huang, T. Jiang, S. Park, J. Xu, X. Wang, Q. Peng, S. Liu, G. Wang and W. Chen, *Adv. Mater.,* 2024, **36**, 2312369.